Effective separation of water-DMSO through solvent resistant membrane distillation (SR-MD)

Yujun Zhang[1,2,3], Jeng Yi Chong[2], Rong Xu[4], and Rong Wang[2,3,*]

[1] Interdisciplinary Graduate Programme, Graduate College, Nanyang Technological University, Singapore 637553, Singapore

[2] Singapore Membrane Technology Centre, Nanyang Environment and Water Research Institute, Nanyang Technological University, Singapore 637141, Singapore

[3] School of Civil and Environmental Engineering, Nanyang Technological University, Singapore 639798, Singapore

[4] School of Chemical and Biomedical Engineering, Nanyang Technological University, Singapore 637459, Singapore

* Email address: rwang@ntu.edu.sg

Graphical abstract

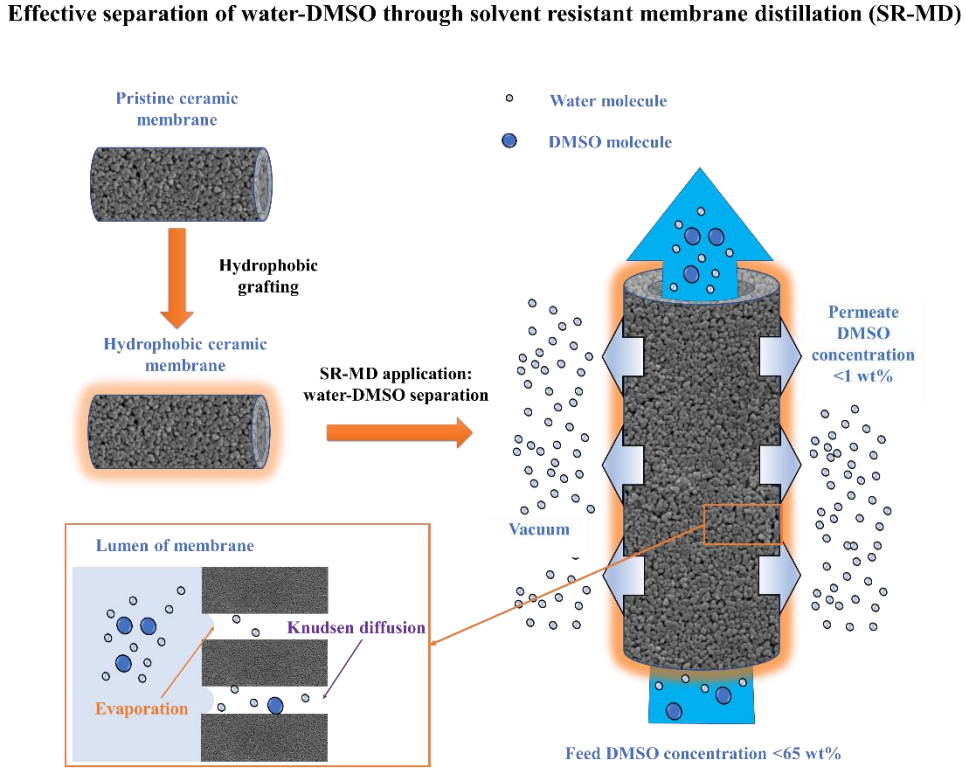

Abstract

The treatment of organic waste or wastewater with high organic solvent content has been challenging in industries as it cannot be done effectively using conventional wastewater treatment technologies such as biodegradation and advanced oxidation process. Solvent resistant membrane distillation (SR-MD) was proposed as an energy-efficient alternative to treat these waste streams but its application is hampered by the lack of solvent-resistant membranes, and there is a research gap in studying the feeds with water-solvent mixtures. In this work, ceramic tubular membranes with different pore sizes and structures were molecularly grafted with 1H,1H,2H,2H-perfluorodecyltriethoxysilane to obtain hydrophobic ceramic membranes for SR-MD. The modified membranes exhibited excellent hydrophobicity and solvent resistant properties, and they were tested for SR-MD performance with a wide range of dimethyl sulfoxide (DMSO) feed concentrations, from 3.5 to 85 wt%. The membranes exhibited a high DMSO rejection of >98 % and the separation factor of >170, with permeation flux >4.4 kg m^{-2} h^{-1} when the DMSO concentration in feed was below 65 wt%. The separation performance was found strongly dependent on the evaporation step and the vapour-liquid equilibrium near the interface. The DMSO rejection was also comparable to pervaporation while the permeation flux was much higher at the feed concentration of 50%. This study establishes the strategy of using SR-MD as a promising membrane process in treating complex industrial wastes with high organic solvent content.

Keywords: Solvent resistant membrane distillation; Water-DMSO separation; Ceramic membranes; Hydrophobic modification; Industrial wastes.

1. Introduction

Organic solvents have been widely used in chemical and pharmaceutical industries for chemical syntheses and product purification (Firestone and Gospe, 2009). The solvents normally cannot be reused after one process cycle without a proper treatment as a high solvent purity is required in most of the processes (Seyler et al., 2006). Therefore, a large amount of organic wastes is generated, and many of these waste streams also contain a significant amount of water. The treatment of organic waste or wastewater with high organic solvent content is challenging as it cannot be done effectively using the conventional chemical or biological methods while the incineration of the waste is not a green pathway.

A typical example is dimethyl sulfoxide (DMSO), which is considered as a comparatively green dipolar aprotic organic solvent because of its low toxicity and good stability (Alder et al., 2016; Xiang et al., 2017). DMSO has been frequently used as a reactant or a reaction medium in the production of pharmaceuticals due to its strong solubility to numerous chemical compounds and good miscibility with many organic solvents and water (Mountford, 2010). However, high concentration of DMSO remaining in the pharmaceutical waste streams is often a challenge to the conventional sewage plants. Both chemical and biological treatments carry their drawbacks: the advanced oxidation process such as Fenton oxidation is costly while the biological treatment is inhibited by the toxic intermediate products and releases unpleasant odour from dimethyl sulfide (Cheng et al., 2009; He et al., 2011). In fact, wastewater with high DMSO content is difficult to be treated in bioreactor because of the biological effect caused by the invasion of DMSO into microorganisms (Smallwood, 2002). The upper limit of DMSO concentration for microbial acclimation in biological process is often reported in the range of 0.10-0.15 wt% (Cheng et al., 2019; Hwang et al., 2012; Yang and Myint, 2003). Meanwhile, incineration is another

common method used to treat these wastes but it has a large carbon footprint and a risk of releasing harmful gases and particulates into the atmosphere (Chea et al., 2020, Seyler et al., 2006). For these issues, the separation of solvent-water mixtures is important to reduce the volume and improve the treatability of solvent-containing waste streams.

Distillation is a common industrial process to separate water and organic solvents with high water miscibility (Kolesnichenko et al., 2019; Ravikumar et al., 2013; Smallwood, 2002). In this process, the feed is heated to a temperature close to the boiling point and a huge amount of energy is required for this conventional separation process. Sometimes, more than one column may be required to achieve desirable product quality. In the case of water-DMSO mixtures, the reboiler temperature of distillation column was reported to be around 120-150 ℃ even when operating under vacuum (Horváth et al., 2017). In addition, the high temperature in distillation may accelerate the hydrolysis of some solvents such as dimethyl formamide and dimethylacetamide, where the hydrolysed products can result in azeotrope problem to the distillation process (Smallwood, 2002). Therefore, an energy efficient separation process is highly desirable to treat organic waste streams that contain water and organic solvents. The separation process can reclaim clean water, recycle valuable solvents or concentrate the waste streams for secondary treatment. Membrane-based separation is an emerging technology that has been widely used in wastewater treatment. However, the commonly used pressure-driven membrane process could not separate water-solvent mixtures effectively due to the similar size between water and solvents, and the high osmotic pressure (Fane et al., 2011). Instead, thermally driven membrane processes such as pervaporation (PV) and membrane distillation (MD) could be used.

The PV has been applied to separate water and a wide range of solvents such as alcohols,

aromatic and aliphatic hydrocarbon, etc (Saw et al., 2019). The PV process is governed by selective sorption and diffusion of species via non-porous membranes and it has an unique strength in separating azeotrope mixtures or mixtures with close boiling points (Mountford, 2010). Generally, organophilic PV membranes favour the permeation of organic solvents, enabling the extraction of solvents, while hydrophilic PV membranes are suitable to reclaim water from water-solvent mixtures. Hydrophobic PV membranes made of cross-linked poly(dimethyl siloxane)–poly(methyl hydrogen siloxane) were reported to remove DMSO from water. A separation factor of 57 can be achieved at 70 ℃ for feed organic concentration of 10 wt%, while the DMSO flux was 0.5 kg m^{-2} h^{-1} (Hosseini and Ameri, 2017). On the other hand, perfluoropolymer-based membranes were studied for the dehydration of DMSO aqueous solution (Tang and Sirkar, 2012). A separation factor over 1000 was reported for the dehydration of 90 wt% DMSO at 30 °C, but the water permeation flux was only 0.0098 kg m^{-2} h^{-1}. As it can be seen, PV membranes often have low permeation flux as the mass transfer is restricted by the low diffusion rate in the dense membranes.

In fact, MD is also a potential membrane technology for separating water-solvent mixtures. Porous hydrophobic membranes are used in the MD process and the permeation was driven by the vapour pressure gradient across the membrane. This non-isothermal membrane process has been extensively studied to reclaim water from various aqueous effluents, including saline water (Deka et al., 2019), radioactive wastewater (Jia et al., 2018), produced water (Chew et al., 2019) and blackish groundwater (Dao et al., 2016). In addition to separating water from non-volatile compounds like inorganic salts, the application of MD can be further expanded to separating water-solvent mixtures based on their difference in vapour pressure. It can be used to separate water from solvents with a high boiling point such as dimethylacetamide (165 °C), DMSO (189 °C) and N-methyl-2-pyrrolidone (202 °C),

as they have a lower vapor pressure compared to water. For instance, the vapour pressure of pure DMSO is only 0.7 kPa while that of water is 19.9 kPa at 60 ℃ (Nishimura et al., 1972). Thus, the vapour condensed subsequently on the permeate side of the MD membrane will have a low DMSO proportion.

In order to successfully utilize solvent resistant membrane distillation (SR-MD), hydrophobic membranes with an excellent chemical stability are required. Among all the polymeric membranes, polytetrafluoroethylene (PTFE) and polypropylene (PP) membranes have strong chemical resistance and high hydrophobicity. Gupta et al. recently developed carbon nanotube immobilized PTFE membranes for the separation of 5-15 vol% isopropyl alcohol (IPA) from an aqueous solution via sweeping gas MD. IPA with a higher vapour pressure permeated through the membranes faster but the separation factor was fairly low, below 13 due to the small difference in the vapour pressure for IPA and water (Gupta et al., 2018). Besides that, PP membranes were applied in the dehydration of n-methyl-2-pyrrolidone (NMP) through vacuum MD (VMD). The membranes exhibited a high water permeation flux of 9.5 L m^{-2} h^{-1} and a rejection of 98 % when the feed contained 10 wt% NMP at 80 ℃ (Shao et al., 2014). Despite its potential in separating solvent-water mixtures, SR-MD processes are less studied as compared to the PV because of the limited availability of SR-MD membranes. Both PTFE and PP membranes with appropriate pore sizes are difficult to fabricate using common membrane fabrication techniques (Feng et al., 2018; Tan and Rodrigue, 2019b). Furthermore, the stability of the polymeric membranes has not been extensively studied and the solvent concentration range tested by far was relatively narrow.

In comparison, ceramic membranes have natural advantages for SR-MD because of their

intrinsic solvent resistant property and good stability in harsh environment, which means they hardly swell or dissolve in organic solvents like polymeric membrane substrates (Chong and Wang, 2019; Marchetti et al., 2014). However, hydrophobic modification is necessary to transform their hydrophilic nature resulted from the rich hydroxyl groups on the membrane surface. Surface grafting is the most commonly used method to modify the surface functional groups of ceramic membranes and many compounds have been previously studied. Among them, fluoroalkylsilane (FAS) is widely used because of the low surface energy of fluoroalkyl compounds (Lu et al., 2019). The FAS compound consists of three hydrolysable groups which can react with hydroxyl groups on ceramic membranes to form strong covalent bonds, and a fluoroalkane chain that can provide hydrophobic character to the membranes (Wei and Li, 2009). Hendren et al. studied ceramic membranes modified by FAS, trichloromethylsilane and trimethyl chlorosilane and they found that FAS modified membrane had a higher flux and better resistance to chlorine (Hendren et al., 2009). Compared to other silane agents without fluorocarbon chain or with a short fluoroalkyl chain, a FAS agent with a longer fluoroalkyl chain imparts better wetting-resistance property to the anodized aluminium oxide membranes (Li et al., 2020). Modified hydrophobic ceramic membranes have been studied for various applications such as MD (Hubadillah et al., 2019b), membrane contactor (Abdulhameed et al., 2017; Lin et al., 2016) and ultrafiltration (Ke et al., 2013). For MD application, hydrophobic ceramic membranes were used for desalination, heavy metal removal as well as VOC removal (Cerneaux et al., 2009; Chen et al., 2018; García-Fernández et al., 2017; Huang et al., 2018; Hubadillah et al., 2019a; Kujawa et al., 2019). Kujawski et al. applied modified ceramic membranes to separate dilute ethyl acetate solution, with a concentration up to 4 wt% (Kujawski et al., 2016). The performance of MD was found to be comparable with PV and the separation factor of ethyl acetate was in the range of 32-60. Besides separating light solvents, hydrophobic ceramic

membranes can potentially be used to separate water from heavy solvents through SR-MD. Nevertheless, the application of SR-MD in a broader solvent concentration and for a longer operating time is still understudied.

In this work, we proposed SR-MD as a novel and effective alternative for separating water from solvents with high boiling points. DMSO was selected in this study because of its relatively low toxicity and increasing use in the industry (Alder et al., 2016; Xiang et al., 2017). Hydrophobic ceramic membranes were modified by grafting FAS onto the substrates, and then their performance in water-DMSO separation was examined by a series of VMD experiments. The effects of feed concentration, temperature and membrane structure were studied in order to understand the separation and transport mechanisms in the SR-MD process. Moreover, a commercial PV membrane was used to separate the water-DMSO feed stream and the results were compared with the counterparts of the SR-MD process. This study aims to demonstrate the effectiveness of SR-MD in separating water-DMSO mixtures over a wide range of DMSO concentrations and facilitate SR-MD applications for other water-solvent systems associated with high boiling point solvents.

2. Experimental

2.1. Materials and Chemicals

Three types of alumina ceramic tubular membranes from Coorstek B.V. (Netherlands) were used as the membrane substrates. They were named as 20-ASY, 200-ASY, 200-SYM according to their pore size (20 or 200 nm) and matrix structures (symmetric or asymmetric) as illustrated in Fig.1. The alumina substrates have an average outer diameter of 4.5 mm and an average inner diameter of 3 mm. Hydrophobic PTFE hollow fibre membranes were

kindly supplied by a commercial company and Hybrid Silica HybSi® AR tubular membranes were purchased from Pervatech B.V. (Netherlands). They were tested for MD and PV as a comparative study. DMSO was purchased from Merck Millipore (Singapore). 1H,1H,2H,2H-perfluorodecyltriethoxysilane ($C_{16}H_{19}F_{17}O_3Si$, 97%) (FAS-F17), methanol (CH_3OH, ≥99.9%), were bought from Sigma-Aldrich (Singapore). All chemicals were used as received. Deionized water was produced by a Milli-Q® system of Merck Millipore (USA).

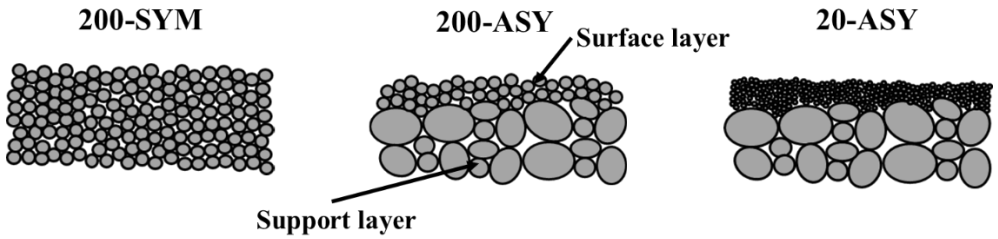

Fig. 1. Schematic of three membrane substrates.

2.2. Hydrophobic grafting of ceramic membranes

The hydrophobic grafting of ceramic membranes is similar to the method reported by other research groups (Koonaphapdeelert and Li, 2007; Kujawski et al., 2007). Firstly, the virgin ceramic membranes were immersed in an ultrasonic water bath for at least 10 min to remove contaminants beforehand. After drying in an oven at 60 ℃ for overnight, the ceramic membranes were then immersed into the grafting solution at 30 ℃ for 2 h, which was prepared by dissolving 2 wt% FAS-F17 in methanol. Then, the membranes were washed in an ultrasonic methanol bath followed by drying in air for 1 h and in an oven at 110 ℃ for 1 h. After taking out from the oven, the same grafting and drying processes were conducted once again to enhance the grafting efficiency. The modified membranes were named as 20-mASY, 200-mASY and 200-mSYM accordingly. The schematic of grafting reaction among the FAS-F17 molecules and ceramic membranes is shown in Fig.2.

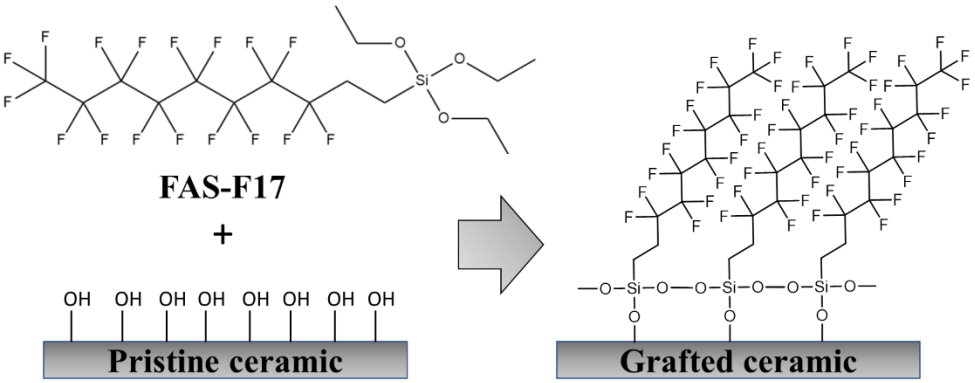

Fig. 2. Schematic of grafting reaction.

2.3. Membrane characterizations

The morphologies of the pristine and modified membranes were characterized by a field emission scanning electron microscope (FESEM, JSM-7200F, JEOL, Japan). The measurement of membrane surface porosity was calculated based on the graph of surface morphology with a magnification of 30,000 times. The inner surface roughness of modified membranes was captured by an atomic force microscope (AFM, NX-100, Park Systems, Republic of Korea) through a non-contact mode. The average pore size and distribution of the membranes were tested by a capillary flow porometer (CFP 1500A, Porous Material. Inc., USA). IPA was used to fill the membranes pores before measurement and nitrogen was used as the pressurised gas to replace the entrapped IPA. In order to examine the grafting reaction occurred on ceramic membranes, the 20-ASY and 20-mASY were tested by X-ray photoelectron spectrometer (XPS, AXIS Supra, Kratos Analytical, Japan) with monochromatic Al-Kα X-ray source (h_v = 1486.6 eV).

The water contact angles (WCA) and solvent contact angles (SCA) of the modified membranes were tested through the sessile drop method by a goniometer (Contact Angle System OCA 15EC, DataPhysics, Germany). Water or pure DMSO droplets were dropped

onto the inner surface of membranes and then the droplets were allowed to stabilize for 3 min before measurement. Afterwards, the display was captured by a camera and the contact angles were defined by the tangent lines of the droplet and the inner circle of membranes. In addition, to evaluate the linkage stability of the hydrophobic chains on the membranes, the contact angles tests were performed after the modified membranes were immersed in pure DMSO at room temperature for 14 and 30 days, respectively.

Liquid entry pressure (LEP) was tested in order to evaluate the entry pressure of feed liquid flooding the membrane pores. LEP_w and LEP_s indicate the entry pressure of water and pure DMSO, respectively. The measurement of LEP was performed in a dead-end configuration where the hollow fibre was connected to a pressure vessel filled with water or DMSO. During the tests, the pressure supplied by compressed N_2 gas was increased with 2 psi every 5 min. Rose bengal was used to stain the tested liquid to give it red colour. When the first drop of water or DMSO appeared on the outer surface of ceramic membranes, the pressure was recorded as the LEP_w and LEP_s, respectively.

2.4. VMD performance tests in water/DMSO solution

A series of VMD tests were conducted on the modified ceramic membranes and the diagram of the setup used is shown in Fig.3. Membrane modules with an effective length of 0.18 m were used in this study. During the VMD tests, the feed solution was heated up to 60 ℃ in a heating jacket tank and circulated by a peristaltic pump (Masterflex, Cole-Parmer, USA) with a flow rate of 170 ml min^{-1} through the lumen of the membranes. A vacuum condensation system was applied in the shell side of the membranes to control the vacuum level at 5 kPa. The generated permeate stream was extracted from the system by a vacuum

pump (RV3, Edwards, UK) and was condensed in a glass condenser cooled by liquid nitrogen.

The collected product was weighted by a mass balance and its DMSO concentration was measured by a gas chromatography equipped with a flame ionization detector (GC-FID) (7890 GC System, Agilent Technologies, USA). The permeate flux (J) was calculated by Eq. (1):

$$J = \frac{m}{A \cdot \Delta t} = \frac{m}{\pi \cdot d \cdot l \cdot \Delta t} \quad (1)$$

where m is the mass of the collected product, A is the effective area of the membrane, Δt is the time interval, d is the inner diameter of the membrane, l is the effective length of membrane contacting feed stream.

The separation performance was evaluated by DMSO rejection (R) and separation factor (α), which were presented as Eq. (2) and Eq. (3), respectively:

$$R = \left(1 - \frac{C_p}{C_f}\right) \times 100\% \quad (2)$$

$$\alpha = \frac{y_w / y_{sol}}{x_w / x_{sol}} \quad (3)$$

where C_p and C_f are the DMSO concentrations of the permeate and the feed stream, y_w and y_{sol} are the weight fractions of water and DMSO in permeate, x_w and x_{sol} are the weight fractions of water and DMSO in feed, respectively.

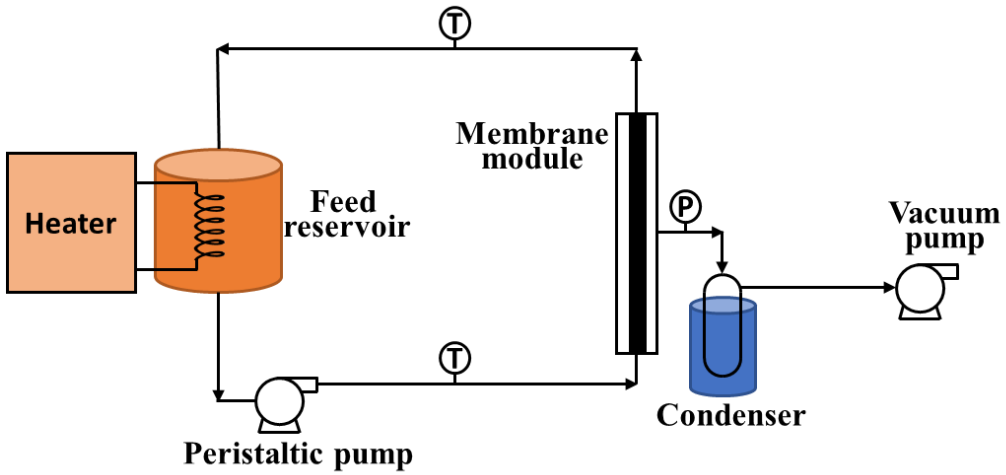

Fig. 3. Schematic of SR-MD experimental setup.

3. RESULTS AND DISCUSSION

3.1. Surface hydrophobic modification of ceramic membranes

Three types of ceramic tubular membranes were used as the substrate: 20-ASY, 200-ASY and 200-SYM, and their pristine properties were first examined before the hydrophobic modification. Figs. 4a and 4b show the characterization of their pore sizes. The 200-SYM and 200-ASY membranes have an average pore size of 228 and 218 nm, respectively, and a fairly narrow pore size distribution. The 20-ASY membrane has a much smaller average pore size, which is hardly measured using the gas-liquid porometry. Instead, the molecular weight cut-off (MWCO) was evaluated by measuring the dextran rejection. The 20-ASY membrane has an MWCO of 94 kDa, and the pore size was estimated to be about 12.8 nm (Ren et al., 2006). Fig.4c shows their structure characteristics: the 200-SYM membrane has a homogeneous pore structure while the 200-ASY and 20-ASY membranes have a surface layer of about 20 and 10 μm, respectively.

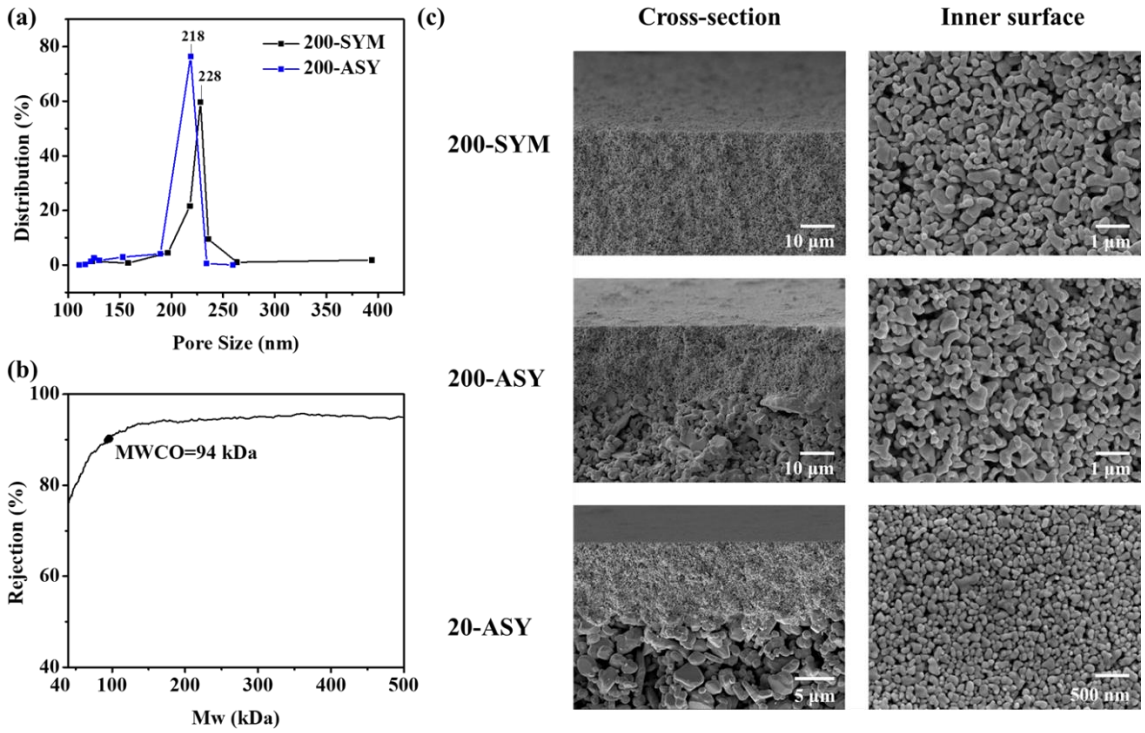

296

297 **Fig. 4.** (a) Pore size distribution of the 200-ASY and 200-SYM membranes obtained using the gas-
298 liquid porometry. (b) MWCO of the 20-ASY membranes. (c) FESEM images of the cross-section
299 and inner surface morphologies of three ceramic substrates.

300

301 The inner surface morphologies of the modified membranes, 200-mSYM, 200-mASY and
302 20-mASY are shown in Fig.5. Compared with the pristine membranes shown in Fig.4c, it
303 can be concluded that the surface morphologies had no significant change after the chemical
304 grafting, as the grafting step only imparted a molecular layer of perfluorinated chains to the
305 membrane surface. Similar observations were reported in previous studies associated with
306 FAS-F17 grafting (García-Fernández et al., 2017; Koonaphapdeelert and Li, 2007; Zhong
307 et al., 2017).

308

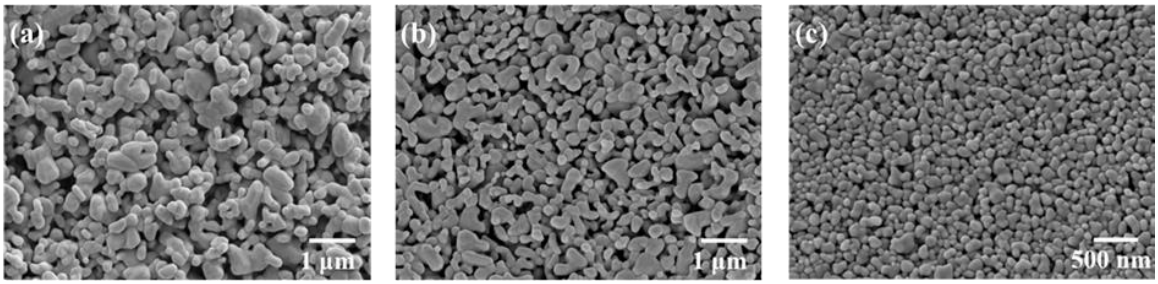

Fig. 5. FESEM images of the inner surface morphologies of the (a) 200-mSYM, (b) 200-mASY, and (c) 20-mASY membranes.

XPS scan was carried out to analyse the elements on the surfaces of the 20-ASY, 20-mASY and 20-mASY-30d membranes. The 20-mASY-30d refers to the sample that has been immersed in pure DMSO for 30 days to evaluate the stability of the hydrophobic modification. As shown in Fig. 6, the 20-mASY membrane spectra clearly shows the characteristic peaks of silicon (Si) and fluoride (F) in addition to carbon ©, oxygen (O) and aluminium (Al), while the 20-ASY membranes are lack of Si and F element. It suggests the successful grafting of FAS-F17 (Koonaphapdeelert and Li, 2007). For the O signals, both Si-O bonds and oxygen in Al_2O_3 lattice can be detected at the range of 531.6 and 533.2 eV, respectively. Furthermore, the 20-mASY-30d membrane has similar characteristic peaks and spectrum as the 20-mASY membrane, indicating good stability of the hydrophobic grafting.

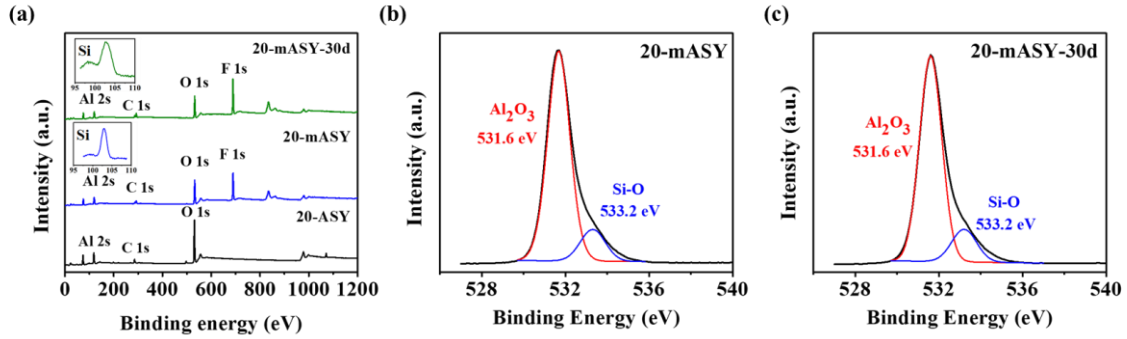

Fig. 6. (a) XPS spectra of the 20-ASY membranes, 20-mASY and 20-mSYM-30d membranes. (b)

O signal of 20-mASY membranes, (c) O signal of 20-mASY-30d membranes.

To determine the surface wettability of the grafted membranes, the contact angles of the membranes were tested and the results are depicted in Fig. 7. It can be seen that the newly modified (0 d) 200-mASY and 200-mSYM membranes have similar WCA >150° and SCA >118°. The lower SCA was ascribed to the lower surface tension of DMSO compared to water (Lide, 2004). Meanwhile, the 20-mASY membrane possesses slightly smaller contact angles than the membranes with larger pore sizes but still shows high hydrophobicity. Though the grafting method used in all three membranes was identical, the difference in the apparent contact angles of hydrophobic surfaces could be contributed by the difference in surface roughness. Table 1 shows the surface roughness parameters of three modified membranes obtained from AFM. The 200-mASY and 200-mSYM membranes have much higher surface roughness, which can contribute to higher apparent contact angles than the 20-mASY membranes. Moreover, the grafted membranes also show good stability in solvent environment, evidenced by the stable contact angles after immersing in pure DMSO for 14 and 30 days. Although there were slight decrements, all modified membranes maintained good hydrophobicity, with WCA >144° and SCA >110° after 30 days.

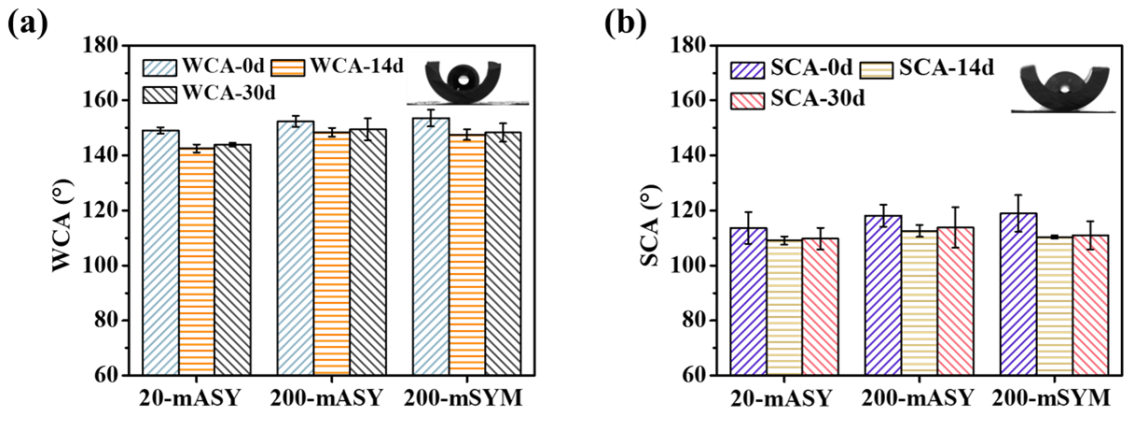

Fig. 7. (a) WCA and (b) SCA of the 20-mASY, 200-mASY and 200-mSYM membranes submerging in DMSO for 0, 14 and 30 days.

The results of LEP_w and LEP_s in Table 1 are in good agreement with the contact angle tests. Before hydrophobic grafting, the ceramic membranes are extremely hydrophilic and both water and DMSO would disperse and penetrate into the pores quickly. However, after the grafting process, the modified membranes possess high LEP_w >30 psi and LEP_s >12 psi, which are much higher than the operating pressure in SR-MD. The good hydrophobicity and high liquid entry barrier can prevent the modified membranes from being wetted by the feed solution, especially when the feed contains high concentration of solvent.

Table 1. Contact angles and liquid entry pressures of grafted membranes.

Membranes	LEP_w (psi)	LEP_s (psi)	Surface roughness parameters	
			R_a[a] (nm)	R_q[b] (nm)
20-mASY	39.5±0.7	12.9±2.4	15.4	19.3
200-mASY	35.9±1.3	12.2±0.4	86.3	109.3
200-mSYM	31.9±3.5	15.2±3.5	126.8	157.9

[a] Average roughness; [b] Root-mean-square roughness

3.2. VMD performance in water-DMSO system

3.2.1 Feed stream with various DMSO concentrations

To study the feasibility of applying the modified ceramic membranes for SR-MD to separate water-DMSO mixtures, the 200-mSYM membranes were first tested with 3.5-85 wt% DMSO feed streams at 60 ℃. As depicted in Fig. 8a, the membrane showed high permeate flux of 7.3 kg m^{-2} h^{-1} at DMSO concentration of 3.5 wt% and the rejection could reach as high as 99.7%. However, both the permeate flux and the solvent rejection decreased with increasing DMSO concentration in the feed. The permeate flux and DMSO rejection was only 1.7 kg m^{-2} h^{-1} and 88.4%, respectively when feed DMSO concentration was 85 wt%.

Fig. 8b indicates the impact of feed DMSO concentration on the permeate purity and the separation factor. Generally, when DMSO in the feed stream became more concentrated, the DMSO concentration in the permeate increased slightly, too. This trend became more distinct when the DMSO concentration in the feed was higher than 65 wt%. As for the separation factor, it reached the best value of 284.4 at 3.5 wt% and remained fairly constant at about 170 when the feed DMSO concentration was between 20 and 65 wt%. Nevertheless, it decreased significantly when the feed concentration was higher than 65 wt%.

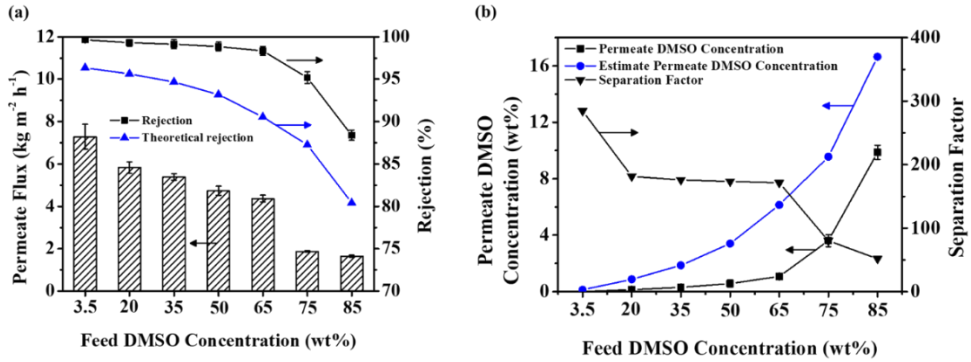

Fig. 8. VMD performances of the 200-mSYM membranes (T_f=60 °C, P=5 kPa, Q_f=170 ml min^{-1}): (a) Flux and DMSO rejection vs. different feed DMSO concentrations. (b) Permeate DMSO concentration and Separation factors vs. different feed DMSO concentrations (theoretical values were obtained based on the Raoult's law).

To understand the behaviours of water and DMSO permeation through the membranes, the transport mechanisms of water and DMSO need to be analysed. During the MD separation process, a vapour-liquid interfaces was formed on the membrane surface, as illustrated in Fig. 9. The feed solution underwent an evaporative phase change near the pore entrance and the vapour transported across the membrane, under the effect of the partial pressure difference, $P_1 - P_0$. Here, P_0 was close to zero because of the applied vacuum and the vapour permeation was highly dependent on the partial pressure near the vapour-liquid interface.

Different from VMD in desalination where the solute is non-volatile, both water and DMSO will evaporate at the vapour-liquid interface. Nevertheless, the VMD process could still effectively separate water from DMSO because of the considerably higher saturated pressure of pure water, which is 19.9 kPa compared to 0.7 kPa of pure DMSO at 60 ℃ (Nishimura et al., 1972). However, when the DMSO concentration increased in the feed solution, the partial pressure of DMSO near the interface increased too, leading to the lower rejection. At the same time, the total vapour pressure of the mixture decreased as the proportion of water in the feed became smaller, resulting in the flux reduction.

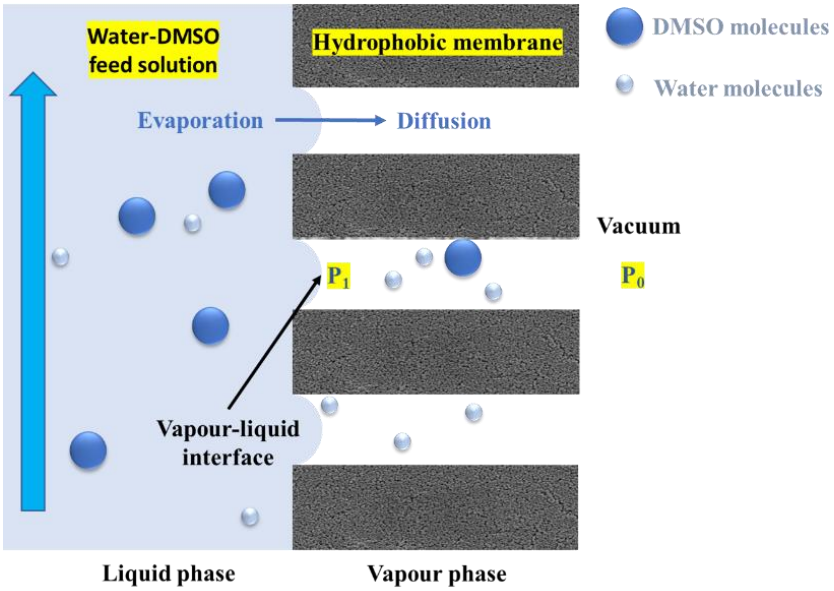

Fig. 9. Schematic of transport mechanisms.

To evaluate the separation performance of VMD, theoretical values of DMSO concentration in permeate and DMSO rejection were estimated based on the Raoult's law by assuming the gas mixture was ideal. The vapour pressure of the pure substance was calculated from Antoine empirical equation. The DMSO mass composition of the permeate can be obtained by Eq. (4) and the rejection was then calculated using Eq. (2).

$$C_{p,est} = \frac{X_{sol}P^*_{sol}M_s}{X_{sol}P^*_{sol}M_s + X_w P^*_w M_w} \quad (4)$$

where X_{sol} and X_w are the liquid mole fraction, P^*_{sol} and P^*_w are the vapour pressure of pure substance, M_s and M_w are the molecular mass of DMSO and water, respectively. Accordingly, when the feed DMSO concentration increases from 3.5 to 85 wt%, the DMSO component in the vapour phase will increase from 0.1 to 16.6 wt% and the DMSO rejection will decrease from 96.4 to 80.4%. Nonetheless, the actual DMSO rejection in the experiments was much higher than the estimation, only reduced from 99.7 to 88.4 wt%.

To understand the reason behind, the diffusion of vapour molecules in the membrane pores should be considered, in addition to the evaporation of feed stream at the interfaces. In the case of VMD, the mean free path of transporting molecules was much higher than the membrane pore sizes. Thus, the diffusion phase was dominated by the Knudsen model which emphasizes the interactions between molecules and membrane pore walls (Schofield et al., 1990). Knudsen diffusion favours the transport of smaller molecules (water) so it has a positive effect on the transportation of water. Although the hydrophobic interaction was weak in gas/vapour phase, the hydrophobic tails of DMSO molecules may still have affinity to the hydrophobic membrane walls and parts of DMSO may be attached on the membrane surface during the collision, and thus slowing down the transport to the permeate side. As a result, the DMSO rejection in the VMD process could exceed the estimated value. The extent of transcendence would be even higher if the tortuosity of the membrane pores was considered.

3.2.2 Effects of feed temperature and membrane structure

To explore the impact of the feed temperature on the membrane performance, VMD tests

were carried out with a 50 wt% DMSO feed solution at temperature ranging from 30 to 60 ℃. Three different types of membranes: 200-mASY, 200-mSYM and 20-mASY were tested and the effects of membrane pore size and structure were also studied. As shown in Fig. 10a, the permeation fluxes of all three membranes improved consistently with the increasing temperature. The 20-mASY exhibited the highest permeation flux among them, where the flux increased from 1.5 kg m^{-2} h^{-1} at 30 °C to 6.9 kg m^{-2} h^{-1} at 60 ℃. The increase of permeation flux could be explained by the higher vapour pressure generated at high temperature, subsequently rendering a higher driving force of mass transfer. At the same time, all three membranes maintained a high rejection (>98%) of DMSO, with a separation factor higher than 105. As discussed in the previous section, the rejection of DMSO highly depends on the vapour pressure of both water and DMSO at the vapour-liquid interface. For 50 wt% liquid mixture, the partial pressure of DMSO increases from 0.02 to 0.1 kPa, while the partial pressure of water increases from 3.5 to 16.1 kPa when the temperature rises from 30 to 60 ℃ (Nishimura et al., 1972). Though the percentage of increase in vapour pressure of DMSO was higher than water, the vapour pressure was still much lower than water and therefore a high rejection of DMSO could still be maintained.

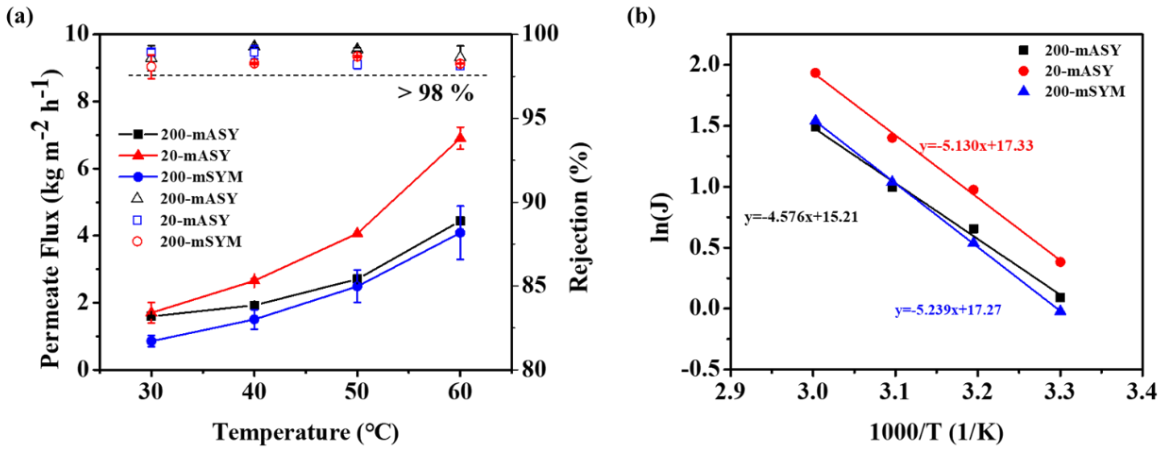

Fig. 10. Effect of feed solution temperature on the VMD permeate flux of the 200-mASY, 200-

mSYM and 20-mASY membranes (C_f=50 wt%, P=5 kPa, Q_f=170 ml min^{-1}).

To further understand the effect of temperature, ln(J) versus T^{-1} was plotted in Fig. 10b. The linear relationship indicates that the permeation fluxes increase exponentially with increasing temperature, following the Arrhenius-type equation. The activation energy can be calculated and it ranges from 38.0-43.6 kJ/mol. The activation energy is a combination of the enthalpy of vaporization and energy of diffusion (Huang et al., 2014). Water is the main component in the vapour phase at the vapour-liquid equilibrium, as shown in the rejection data where the concentration of DMSO was less than 1 wt% in the permeate. The enthalpy of vaporization was mainly contributed by water and the heat of evaporation of water was 42.48-43.78 kJ/mol in this temperature range (Lide, 2004). The similar value between the enthalpy of vaporization and activation energy may suggest the predominant effect of the evaporation step in affecting the permeation flux.

There is no significant difference between the performances of the 200-mASY and 200-mSYM membranes even though their matrix structures are different. The 200-mSYM has a similar pore structure across the membrane while the 200-mASY consists of two layers: a top layer with similar structure as the 200-mSYM and the support layer with a larger pore size. The asymmetric structure of 200-mASY did not enhance the permeation flux and the reason could be laid on the fact that the evaporation step near the vapour-liquid interface presented the predominant impact on the permeation rate.

On the other hand, it was found that the 20-mASY membrane exhibited a higher permeation flux compared to the 200-mASY and 200-mSYM membranes, despite its smaller pore size. This can be explained by the higher surface porosity and smaller membrane thickness of the

20-mASY membrane. As the evaporation step had a strong effect on the permeation flux, the total surface area of the vapour-liquid interface may directly affect the total permeation flux. As illustrated in Fig. 11, the inner surface porosity of the 20-ASY membrane is 21.6%, which is higher than the 200-SYM and 200-ASY membranes, allowing a larger vapour-liquid interface for vapour evaporation. Also, the 20-ASY membranes (thickness of 0.75 mm) were 17% thinner than the 200-SYM membranes (thickness of 0.9 mm), which could in turn posed a lower mass transfer resistance to the permeation flux.

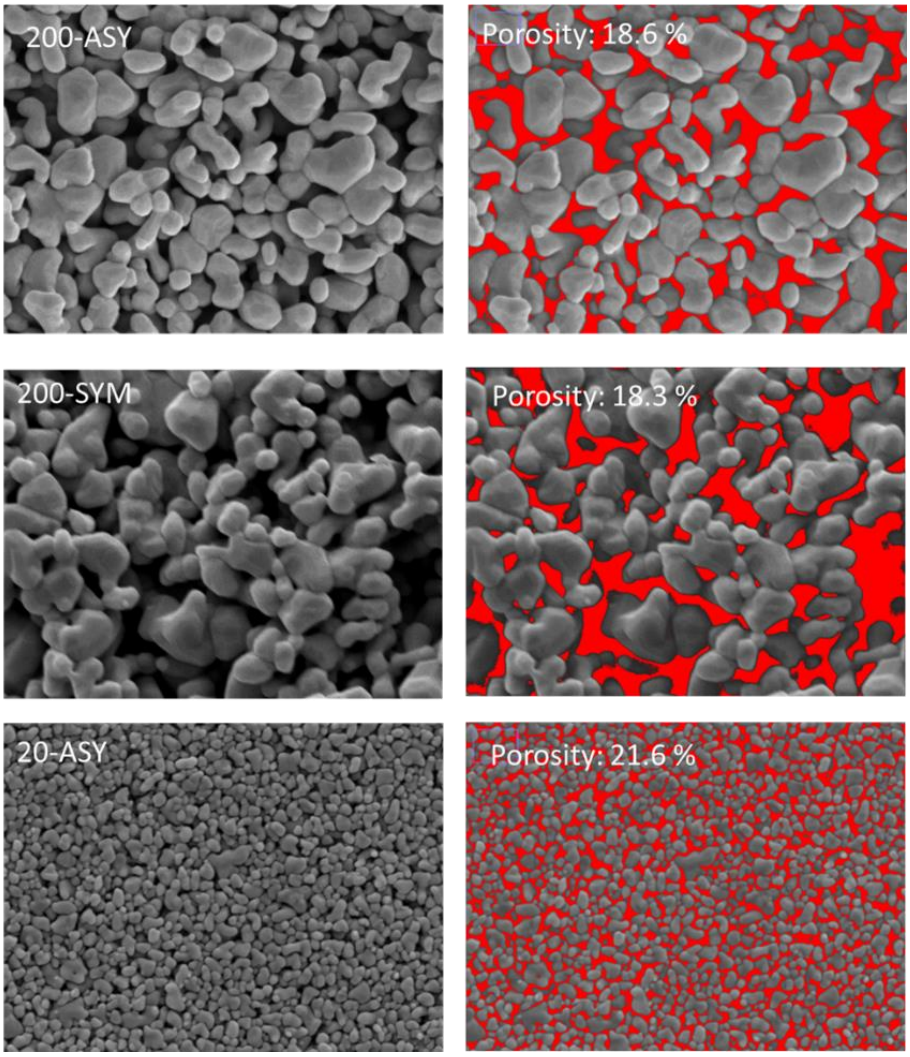

Fig. 11. Surface porosity of the inner surface of 200-ASY, 200-SYM and 20-ASY membranes (pore area is indicated in red colour).

3.2.3 24-hour performance in water-DMSO feed solution

24-hour VMD tests were conducted to study the stability of the membranes in solvent-containing system. The hydrophobic ceramic membranes were prepared through surface functionalization and their stability in MD was highly dependent on the stability of the functionalization layer. As shown in section 3.1, the WCA and SCA of the membranes remained high values even after immersing in DMSO for a month. Besides that, the membranes are more likely to suffer from membrane wetting in VMD compared to direct contact MD because of the pressure gradient across the membranes (Rezaei et al., 2018). If the membranes were wetted by the feed solution, the arc-shaped interface at the pore entrance will no longer be maintained. The liquid would start to permeate through the membranes via a viscous flow and the DMSO rejection would subsequently deteriorate.

During the experiments, the 200-mSYM membranes were fed with 20-75 wt% DMSO and the VMD process was run for 24 hours for each concentration. As shown in Fig.12, the membrane presented consistent performance with no sign of wetting. Though there were some minor fluctuations, the modified membranes were able to maintain an average rejection at higher than 95%. The high rejection reflected that the membrane pores survived from wetting by the feed stream even when the DMSO concentration in the feed was as high as 75 wt%. Also, the permeate flux kept reasonably stable in the whole experiment period, which was in accordance with the results of previous tests. When the DMSO concentrations were lower than 50 wt%, the average flux was higher than 4.7 kg m^{-2} h^{-1}.

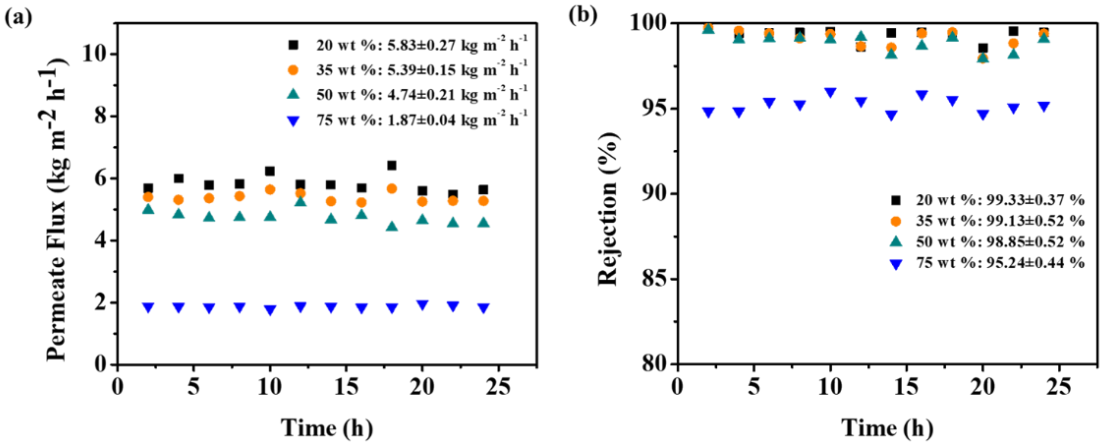

Fig. 12. (a) Permeate flux and (b) DMSO rejection of the 200-mSYM membranes in 20-75 wt% DMSO/water feed stream (T_f=60 °C, P=5 kPa, Q_f=170 ml min^{-1}).

3.3 Separation performance of other types of membranes

Currently there are limited types of membranes that can be used for SR-MD due to the lack of solvent resistance of most polymeric membranes. Commonly used MD membranes such as PVDF membrane fabricated by phase inversion method cannot withstand strong solvents such as DMSO and NMP (Tan and Rodrigue, 2019a). Meanwhile, the PP and PTFE membranes mainly fabricated by melt-spinning, cold-stretching or thermally induced phase separation methods (Tan and Rodrigue, 2019b) can be potentially used for SR-MD because they have both high hydrophobicity and excellent chemical resistance. Therefore, in this study, we also used commercial PTFE hollow fibres for water-DMSO separation. PTFE membrane with similar pore size (bubble point pore size = 361 nm and mean pore size = 112 nm) was tested, and results are shown in Figure 13. The membrane showed a much lower permeation flux (2.6 kg m^{-2} h^{-1}) compared to the modified ceramic membranes at feed concentration of 50 wt%. Furthermore, the membrane started to wet when the feed DMSO concentration was increased to 85 wt%. The fast wetting of PTFE membranes could be due to the large pore size distribution, resulting from the stretching method used in the

membrane fabrication (Tan and Rodrigue, 2019b).

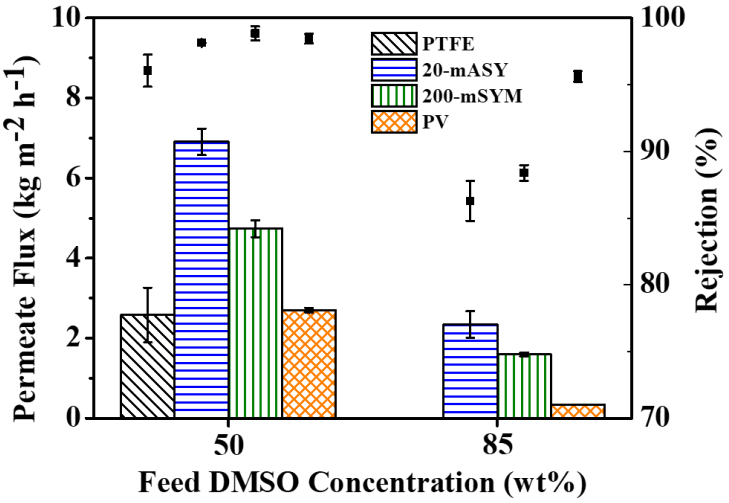

Fig. 13 Comparison of the separation performance of 20-mASY, 200-mSYM and other membranes.

In this study, we also tested the commercial Hybrid Silica HybSi® AR membranes used in the PV process to compare the efficiency of VMD and PV in separating water-DMSO mixtures. As shown in Fig. 13, VMD membranes showed great superiority in permeate flux, which was 156% and 588% higher than that of PV process when treating 50 and 85 wt% DMSO with the 20-mASY membrane, respectively. The DMSO rejection of VMD was as great as PV (>98%) when the feed DMSO concentration was 50 wt%. However, when the feed concentration was 85 wt%, the rejection of the 20-mASY and 200-mSYM membranes dropped to 86.3 and 88.4%, respectively, while the rejection of PV remained high at 95.6%. PV is hardly restricted by the vapour-liquid equilibrium at the interface, and the more selective sorption step contributed to the high DMSO rejection at high feed concentration (Guo et al., 2004). However, the permeation flux was significantly lower as diffusion through the dense PV membranes was much slower than Knudsen diffusion.

In summary, SR-MD has been demonstrated to be a promising separation process to separate water-DMSO effectively. The modified ceramic membranes exhibited a high permeation flux for a wide range of DMSO feed concentrations, and they also showed rejection higher than 90% when the feed concentration was lower than 85 wt%. Water with low organic content can be produced on the permeate side and it can then undergo a simple secondary purification process for further processing before reuse or discharge. For example, DMSO content in the permeate is smaller than the bioreactor limit (0.1-0.15 wt%) when the DMSO concentration in the SR-MD feed stream is lower than 20 wt%. The permeate product can be sent directly to the bioreactor where DMSO will be degraded completely. At the same time, the SR-MD process can dehydrate and concentrate DMSO in a diluted feed stream, making it more viable for reuse in manufacturing. The application of SR-MD is not limited to water-DMSO separation but can potentially be used to treat wastewater containing other organic solvents that have a high boiling point (>150 °C) like NMP, and some typical degradation-resistant solvents, such as dimethylformamide and dimethylacetamide (Kong et al., 2019; Peng et al., 2018). To give an example, the 20-mASY membrane was tested with a 50 wt% NMP feed stream at 60 ℃ and showed excellent rejection of 96.4±0.3% and separation factor of 53.9±4.2, with high flux of 7.3±0.2 kg m^{-2} h^{-1}. Therefore, the treatment strategy involving SR-MD can be extended to treat more complicated industrial feeds containing various organic solvents.

4. Conclusions

Hydrophilic ceramic membranes were successfully transformed into hydrophobic ones by chemical grafting of FAS-F17, and the analysis showed that the hydrophobic modification was stable even after immersing in pure DMSO over 30 days. The modified ceramic membranes were subsequently used in SR-MD to separate water-DMSO mixtures. The

membranes kept unwetted and showed excellent performance in VMD tests using feed streams with a wide range of DMSO concentrations (3.5-85 wt%). Especially, the separation factor was as high as 284 at feed concentration of 3.5 wt% DMSO and stayed constant at about 170 at feed concentration of 20-65 wt% DMSO.

In comparison, the commercial PTFE MD membranes failed to resist the penetration of feed containing 85 wt% DMSO. Additionally, all the modified ceramic membranes could maintain a rejection higher than 98% when treating 50 wt% DMSO solution, which was at the same level as the commercial PV membrane tested. The permeation flux of 20-mASY membranes was also much higher, 156% and 588% higher than that of PV process when treating 50 and 85 wt% of DMSO, respectively. The separation performance of SR-MD was found strongly dependent on the vapour-liquid equilibrium near the interface, and the permeation flux was predominantly affected by the evaporation step. This study demonstrates that SR-MD can be a promising technique to treat complex wastewater containing organic solvents.

ACKNOWLEDGEMENTS

The authors would like to acknowledge funding support from the Singapore Economic Development Board to the Singapore Membrane Technology Centre, Nanyang Environment & Water Research Institute at Nanyang Technological University, Singapore.

588 **References**

589 Abdulhameed, M.A., Othman, M.H.D., Ismail, A.F., Matsuura, T., Harun, Z., Rahman,
590 M.A., Puteh, M.H., Jaafar, J., Rezaei, M. and Hubadillah, S.K. (2017) Carbon dioxide
591 capture using a superhydrophobic ceramic hollow fibre membrane for gas-liquid
592 contacting process. Journal of Cleaner Production 140, 1731-1738.

593 Alder, C.M., Hayler, J.D., Henderson, R.K., Redman, A.M., Shukla, L., Shuster, L.E. and
594 Sneddon, H.F. (2016) Updating and further expanding GSK's solvent sustainability guide.
595 Green Chemistry 18(13), 3879-3890.

596 Cerneaux, S., Struzynska, I., Kujawski, W.M., Persin, M. and Larbot, A. (2009)
597 Comparison of various membrane distillation methods for desalination using hydrophobic
598 ceramic membranes. Journal of Membrane Science 337(1-2), 55-60.

599 Chen, X., Gao, X., Fu, K., Qiu, M., Xiong, F., Ding, D., Cui, Z., Wang, Z., Fan, Y. and
600 Drioli, E. (2018) Tubular hydrophobic ceramic membrane with asymmetric structure for
601 water desalination via vacuum membrane distillation process. Desalination 443, 212-220.

602 Cheng, H.-H., Liu, C.-B., Lei, Y.-Y., Chiu, Y.-C., Mangalindan, J., Wu, C.-H., Wu, Y.-J.
603 and Whang, L.-M. (2019) Biological treatment of DMSO-containing wastewater from
604 semiconductor industry under aerobic and methanogenic conditions. Chemosphere 236,
605 124291.

606 Cheng, X., Wodarczyk, M., Lendzinski, R., Peterkin, E. and Burlingame, G.A. (2009)
607 Control of DMSO in wastewater to prevent DMS nuisance odors. Water Research 43(12),
608 2989-2998.

609 Chew, N.G.P., Zhang, Y., Goh, K., Ho, J.S., Xu, R. and Wang, R. (2019) Hierarchically
610 Structured Janus Membrane Surfaces for Enhanced Membrane Distillation Performance.
611 ACS Appl Mater Interfaces 11(28), 25524-25534.

612 Chong, J.Y. and Wang, R. (2019) From micro to nano: Polyamide thin film on
613 microfiltration ceramic tubular membranes for nanofiltration. Journal of Membrane
614 Science 587.

615 Dao, T.D., Laborie, S. and Cabassud, C. (2016) Direct As (III) removal from brackish
616 groundwater by vacuum membrane distillation: effect of organic matter and salts on
617 membrane fouling. Separation and Purification Technology 157, 35-44.

618 Deka, B.J., Guo, J.X., Khanzada, N.K. and An, A.K. (2019) Omniphobic re-entrant PVDF
619 membrane with ZnO nanoparticles composite for desalination of low surface tension oily
620 seawater. Water Research 165, 12.

621 Fane, A.G., Tang, C.Y. and Wang, R. (2011) Treatise on Water Science. Wilderer, P. (ed),
622 pp. 301-335, Elsevier, Oxford.

623 Feng, S., Zhong, Z., Wang, Y., Xing, W. and Drioli, E. (2018) Progress and perspectives
624 in PTFE membrane: Preparation, modification, and applications. Journal of Membrane
625 Science 549, 332-349.

626 Firestone, J.A. and Gospe, S.M. (2009) Clinical Neurotoxicology. Dobbs, M.R. (ed), pp.
627 401-414, W.B. Saunders, Philadelphia.

628 García-Fernández, L., Wang, B., García-Payo, M.C., Li, K. and Khayet, M. (2017)
629 Morphological design of alumina hollow fiber membranes for desalination by air gap
630 membrane distillation. Desalination 420, 226-240.

631 Guo, W.F., Chung, T.S., Matsuura, T., Wang, R. and Liu, Y. (2004) Pervaporation study
632 of water and tert-butanol mixtures. Journal of Applied Polymer Science 91(6), 4082-4090.

633 Gupta, O., Roy, S. and Mitra, S. (2018) Enhanced membrane distillation of organic
634 solvents from their aqueous mixtures using a carbon nanotube immobilized membrane.
635 Journal of Membrane Science 568, 134-140.

636 He, S.-Y., Lin, Y.-H., Hou, K.-Y. and Hwang, S.-C.J. (2011) Degradation of dimethyl-
637 sulfoxide-containing wastewater using airlift bioreactor by polyvinyl-alcohol-immobilized
638 cell beads. Bioresource Technology 102(10), 5609-5616.

639 Hendren, Z.D., Brant, J. and Wiesner, M.R. (2009) Surface modification of nanostructured
640 ceramic membranes for direct contact membrane distillation. Journal of Membrane
641 Science 331(1-2), 1-10.

642 Horváth, D., Matolcsy, K., Szita, K. and Zajáros, A. (2017) Life Cycle Sustainability
643 Assessment of DMSO Solvent Recovery from Hazardous Waste Water. Periodica
644 Polytechnica Chemical Engineering 62(3), 305-309.

645 Hosseini, M. and Ameri, E. (2017) Pervaporation characteristics of a PDMS/PMHS
646 membrane for removal of dimethyl sulfoxide from aqueous solutions. Vacuum 141, 288-
647 295.

648 Huang, C.-Y., Ko, C.-C., Chen, L.-H., Huang, C.-T., Tung, K.-L. and Liao, Y.-C. (2018)
649 A simple coating method to prepare superhydrophobic layers on ceramic alumina for
650 vacuum membrane distillation. Separation and Purification Technology 198, 79-86.

651 Huang, K., Liu, G., Lou, Y., Dong, Z., Shen, J. and Jin, W. (2014) A graphene oxide
652 membrane with highly selective molecular separation of aqueous organic solution. Angew
653 Chem Int Ed Engl 53(27), 6929-6932.

654 Hubadillah, S.K., Othman, M.H.D., Ismail, A.F., Rahman, M.A. and Jaafar, J. (2019a) A
655 low cost hydrophobic kaolin hollow fiber membrane (h-KHFM) for arsenic removal from
656 aqueous solution via direct contact membrane distillation. Separation and Purification
657 Technology 214, 31-39.

658 Hubadillah, S.K., Tai, Z.S., Othman, M.H.D., Harun, Z., Jamalludin, M.R., Rahman,
659 M.A., Jaafar, J. and Ismail, A.F. (2019b) Hydrophobic ceramic membrane for membrane
660 distillation: A mini review on preparation, characterization, and applications. Separation
661 and Purification Technology 217, 71-84.

662 Hwang, S., Lin, Y., Chang, Y. and He, S. (2012) Effect of microbial activity on dimethyl
663 sulfoxide degradation in an air-lift bioreactor. WIT Transactions on Ecology and the
664 Environment 163, 403-413.

665 Jia, F., Yin, Y. and Wang, J. (2018) Removal of cobalt ions from simulated radioactive
666 wastewater by vacuum membrane distillation. Progress in Nuclear Energy 103, 20-27.

667 Ke, X., Huang, Y., Dargaville, T.R., Fan, Y., Cui, Z. and Zhu, H. (2013) Modified
668 alumina nanofiber membranes for protein separation. Separation and Purification
669 Technology 120, 239-244.

670 Kolesnichenko, I.V., Goloverda, G.Z. and Kolesnichenko, V.L. (2019) A Versatile
671 Method of Ambient-Temperature Solvent Removal. Organic Process Research &
672 Development 24(1), 25-31.

673 Kong, Z., Li, L., Xue, Y., Yang, M. and Li, Y.-Y. (2019) Challenges and prospects for the
674 anaerobic treatment of chemical-industrial organic wastewater: A review. Journal of
675 Cleaner Production 231, 913-927.

676 Koonaphapdeelert, S. and Li, K. (2007) Preparation and characterization of hydrophobic
677 ceramic hollow fibre membrane. Journal of Membrane Science 291(1-2), 70-76.

678 Kujawa, J., Kujawski, W., Cyganiuk, A., Dumée, L.F. and Al-Gharabli, S. (2019)
679 Upgrading of zirconia membrane performance in removal of hazardous VOCs from water
680 by surface functionalization. Chemical Engineering Journal 374, 155-169.

681 Kujawski, W., Krajewska, S., Kujawski, M., Gazagnes, L., Larbot, A. and Persin, M.
682 (2007) Pervaporation properties of fluoroalkylsilane (FAS) grafted ceramic membranes.
683 Desalination 205(1), 75-86.

684 Kujawski, W., Kujawa, J., Wierzbowska, E., Cerneaux, S., Bryjak, M. and Kujawski, J.
685 (2016) Influence of hydrophobization conditions and ceramic membranes pore size on
686 their properties in vacuum membrane distillation of water–organic solvent mixtures.
687 Journal of Membrane Science 499, 442-451.

688 Li, C., Li, X., Du, X., Zhang, Y., Wang, W., Tong, T., Kota, A.K. and Lee, J. (2020)
689 Elucidating the Trade-off between Membrane Wetting Resistance and Water Vapor Flux
690 in Membrane Distillation. Environmental Science & Technology 54(16), 10333-10341.

691 Lide, D.R. (2004) CRC handbook of chemistry and physics, CRC press.

692 Lin, Y.-F., Ye, Q., Hsu, S.-H. and Chung, T.-W. (2016) Reusable fluorocarbon-modified
693 electrospun PDMS/PVDF nanofibrous membranes with excellent CO2 absorption
694 performance. Chemical Engineering Journal 284, 888-895.

695 Lu, K.J., Chen, Y. and Chung, T.-S. (2019) Design of omniphobic interfaces for
696 membrane distillation – A review. Water Research 162, 64-77.

697 Marchetti, P., Jimenez Solomon, M.F., Szekely, G. and Livingston, A.G. (2014)
698 Molecular separation with organic solvent nanofiltration: a critical review. Chemical
699 reviews 114(21), 10735-10806.

700 Mountford, P. (2010) Green Chemistry in the Pharmaceutical Industry. Dunn, PJ, 145-
701 160.

702 Nishimura, M., Nakayama, M. and Yano, T. (1972) Vapor pressure of pure DMSO and
703 vapor-liquid equilibria in DMSO-H2O system under isobaric conditions. Journal of
704 Chemical Engineering of Japan 5(3), 223-226.

705 Peng, J., Yan, J., Chen, Q., Jiang, X., Yao, G. and Lai, B. (2018) Natural mackinawite
706 catalytic ozonation for N, N-dimethylacetamide (DMAC) degradation in aqueous solution:
707 Kinetic, performance, biotoxicity and mechanism. Chemosphere 210, 831-842.

708 Ravikumar, Y.V.L., Sridhar, S. and Satyanarayana, S.V. (2013) Development of an
709 electrodialysis–distillation integrated process for separation of hazardous sodium azide to
710 recover valuable DMSO solvent from pharmaceutical effluent. Separation and Purification
711 Technology 110, 20-30.

712 Ren, J., Li, Z. and Wong, F.-S. (2006) A new method for the prediction of pore size
713 distribution and MWCO of ultrafiltration membranes. Journal of Membrane Science
714 279(1-2), 558-569.

715 Rezaei, M., Warsinger, D.M., Lienhard, V.J., Duke, M.C., Matsuura, T. and Samhaber,
716 W.M. (2018) Wetting phenomena in membrane distillation: Mechanisms, reversal, and
717 prevention. Water Res 139, 329-352.

718 Saw, E.T., Ang, K.L., He, W., Dong, X. and Ramakrishna, S. (2019) Molecular sieve
719 ceramic pervaporation membranes in solvent recovery: A comprehensive review. Journal
720 of Environmental Chemical Engineering 7(5).

721 Schofield, R.W., Fane, A.G. and Fell, C.J.D. (1990) Gas and vapour transport through
722 microporous membranes. I. Knudsen-Poiseuille transition. Journal of Membrane Science
723 53(1), 159-171.

724 Seyler, C., Capello, C., Hellweg, S., Bruder, C., Bayne, D., Huwiler, A. and
725 Hungerbühler, K. (2006) Waste-Solvent Management as an Element of Green Chemistry:
726 A Comprehensive Study on the Swiss Chemical Industry. Industrial & Engineering
727 Chemistry Research 45(22), 7700-7709.

728 Shao, F., Hao, C., Ni, L., Zhang, Y., Du, R., Meng, J., Liu, Z. and Xiao, C. (2014)
729 Experimental and theoretical research on N-methyl-2-pyrrolidone concentration by
730 vacuum membrane distillation using polypropylene hollow fiber membrane. Journal of
731 Membrane Science 452, 157-164.

732 Smallwood, I.M. (2002) Solvent recovery handbook, CRC Press.

733 Tan, X. and Rodrigue, D. (2019a) A Review on Porous Polymeric Membrane Preparation.
734 Part I: Production Techniques with Polysulfone and Poly (Vinylidene Fluoride). Polymers
735 11(7).

736 Tan, X. and Rodrigue, D. (2019b) A Review on Porous Polymeric Membrane Preparation.
737 Part II: Production Techniques with Polyethylene, Polydimethylsiloxane, Polypropylene,
738 Polyimide, and Polytetrafluoroethylene. Polymers (Basel) 11(8).

739 Tang, J. and Sirkar, K.K. (2012) Perfluoropolymer membrane behaves like a zeolite
740 membrane in dehydration of aprotic solvents. Journal of Membrane Science 421-422, 211-
741 216.

742 Wei, C.C. and Li, K. (2009) Preparation and Characterization of a Robust and
743 Hydrophobic Ceramic Membrane via an Improved Surface Grafting Technique. Industrial
744 & Engineering Chemistry Research 48(7), 3446-3452.

745 Xiang, J.-C., Gao, Q.-H. and Wu, A.-X. (2017) The Applications of DMSO. Solvents as
746 Reagents in Organic Synthesis: Reactions and Applications, 315-353.

747 Yang, P.Y. and Myint, T.T. (2003) Integrating entrapped mixed microbial cell (EMMC)
748 technology for treatment of wastewater containing dimethyl sulfoxide (DMSO) for reuse
749 in semiconductor industries. Clean Technologies and Environmental Policy 6(1), 43-50.

750 Zhong, W., Hou, J., Yang, H.-C. and Chen, V. (2017) Superhydrophobic membranes via
751 facile bio-inspired mineralization for vacuum membrane distillation. Journal of Membrane
752 Science 540, 98-107.
753